RadioGraphics

Normal Doppler Spectral Waveforms of Major Pediatric Vessels: Specific Patterns[1]

Govind B. Chavhan, MD, DNB • Dimitri A. Parra, MD • Andrea Mann, RDMS • Oscar M. Navarro, MD

TEACHING POINTS
See last page

Every major vessel in the human body has a characteristic flow pattern that is visible in spectral waveforms obtained in that vessel with Doppler ultrasonography (US). Spectral waveforms reflect the physiologic status of the organ supplied by the vessel, as well as the anatomic location of the vessel in relation to the heart. In addition, the waveforms may be affected by age- and development-related hemodynamic differences. For example, adults tend to have higher flow velocities, whereas neonates, particularly those born prematurely, have higher resistance to flow, especially in the cerebral and renal vascular beds. As Doppler US is performed with increasing frequency for vascular evaluation in children, the recognition of normal flow patterns has become imperative. Familiarity with the waveforms characteristic of specific veins and arteries in children is important. In addition, an understanding of the hemodynamic factors involved provides a useful basis for interpreting waveform abnormalities.

©RSNA, 2008 • *radiographics.rsnajnls.org*

Teaching Point

Introduction

Blood flow through a vessel is affected by the pressure differential between the ends of the vessel and by resistance presented by the vessel wall (1). Whereas the first factor is determined by cardiac function and the relative position of the vessel in the circulatory system, the latter depends on the physiologic status of the vessel and the demand for blood. In other words, each normal major vessel in the human body has a characteristic flow pattern that is representable in spectral waveforms obtained with Doppler ultrasonography (US) and that reflects both the anatomic position of the vessel and the physiologic need of the organ it supplies (1). Since cardiac function may be considered to exert the same effect on flow through all the vessels, the two main determinants of flow characteristics in a particular vessel are the resistance, which varies according to the physiologic need of the organ, and the distance of the vessel from the heart. Vascular resistance may be altered by physiologic differences or pathologic conditions. Most of the peripheral resistance is offered by arterioles because of changes in the tone of arteriolar muscles (2).

The article begins with a general explanation of the structure and components of the Doppler spectrum, the kinds of information that can be derived from spectral waveforms, and frequently observed patterns of arterial and venous flow. It then describes in detail the characteristic waveforms of blood flow in major pediatric vessels according to their anatomic location. The spectral effects of age- and development-related hemodynamic differences between children and adults are emphasized.

Structure and Components of Doppler Spectra

The Doppler spectrum is a time-velocity waveform that represents variation in intravascular blood flow velocities during the cardiac cycle (2). Time is represented along the horizontal axis, and frequency shift (velocity) is depicted along the vertical axis (Fig 1). The intensity or brightness (also referred to as the gray-scale velocity plot) of the spectral line represents the number of red blood cells that are reflecting the ultrasound beam at each velocity. The width of the spectral

line represents the range of velocities within a vessel. The width may vary during the normal cardiac cycle, narrowing during systole and widening in diastole (2).

The spectral window is the clear black zone between the spectral line and the baseline. Widening of the spectral line and filling of the spectral window is called spectral broadening. Spectral broadening is normally seen in the presence of high flow velocity, at the branching of a vessel, or in small-diameter vessels.

Calculation of Arterial Flow Indexes

The resistive index (RI) can be calculated from spectral measurements by using the equation $RI = (PSV - EDV)/PSV$, where PSV is the peak systolic velocity and EDV is the end-diastolic velocity (1). The pulsatility index (PI) can be calculated by using the equation $PI = (PSV - EDV)/MV$, where MV is the mean flow velocity during the cardiac cycle.

The RI and the PI provide information about blood flow and resistance that cannot be obtained from measurements of absolute velocity alone. The effects of variation in vessel angulation and size are nullified in the calculation of these indexes (1). Various abnormal waveforms may be compared by calculating the RI and PI. Physiologic events that alter vascular resistance and thus affect waveforms include exercise, changes in gravity orientation and stress level, and digestion (1).

Teaching Point

Normal Doppler Flow Patterns

Plug Flow
In plug flow, all the red blood cells move at the same velocity, producing a flat wave front. The Doppler spectrum from this flow pattern is characterized by a narrow spectral line and a clear spectral window, which represent the absence of lower velocities (2). That waveform typically is seen in large arteries, such as the aorta.

Laminar Flow
In laminar flow, peripheral red blood cells move at a slower rate than central red blood cells do, because of friction offered by the vessel wall. This difference in flow velocities produces a parabolic
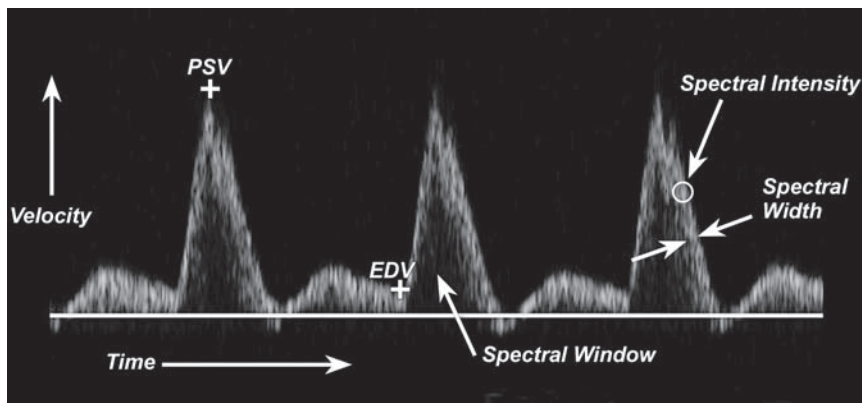
Figure 1. Diagram shows a normal arterial spectrum obtained with Doppler US, the parameters that define it, and the general terms used to describe it. *PSV* = peak systolic velocity, *EDV* = end-diastolic velocity.
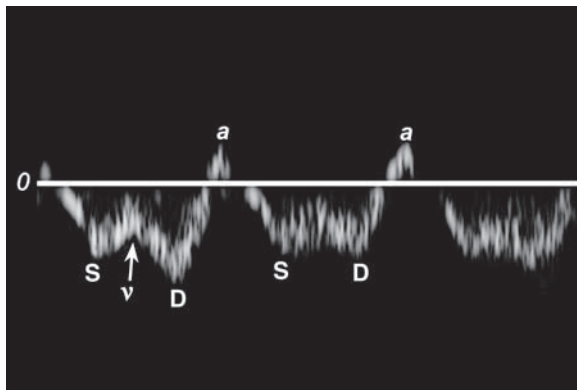

Figure 2. Diagram shows a normal venous spectrum obtained with Doppler US, which includes *a*, S, *v*, and D waves that represent back-pulsations caused by right atrial pressure changes during the cardiac cycle. This flow pattern is most evident in the veins closest to the heart.

wave front. In Doppler US spectra, laminar flow appears as broadening of the spectral line and filling of the spectral window (2). That waveform usually is seen in vessels with a diameter of less than 5 mm.

Turbulent Flow
Turbulent flow consists of a wide range of velocities, includes reversed flow components, and is readily appreciated as multiple colors on color Doppler images. In spectra, a turbulent flow pattern is visible as spectral broadening with components below the baseline. Turbulent flow is considered normal near vessel bifurcations (eg, the carotid bulb) but elsewhere is suggestive of abnormality (2).

Venous Flow Patterns
Normal venous flow is affected by back-pulsations that result from cardiac movements and by phasic changes associated with respiration (3). The visibility of respiratory phases in the venous waveform depends on many factors, including the distance of the vein from the chest. Venous waveforms comprise S, *v*, D, and *a* waves (Fig 2) (3). S is the systolic wave, which results from negative intraatrial pressure with movement of the atrioventricular septum toward the cardiac apex. The *v* wave is the result of positive intraatrial pressure created by overfilling of the right atrium. D is the diastolic wave, which results from negative intraatrial pressure caused by the opening of the tricuspid valve. The *a* wave reflects positive intraatrial pressure during atrial systole. In subsequent sections, the influence of the respiratory phase on each of these waveform components is described according to the anatomic location of the particular vein.

Head and Neck Vessels

External Carotid Artery
This artery supplies the high-resistance vascular bed of the facial muscles. The normal spectrum in this location rises sharply during systole and falls rapidly, approaching zero or descending transiently below the baseline, in diastole (Fig 3a). Normal value ranges in adults include a PSV of 57–87 cm/sec, an EDV of 11–21 cm/sec, and an RI of 0.72–0.84 (4).
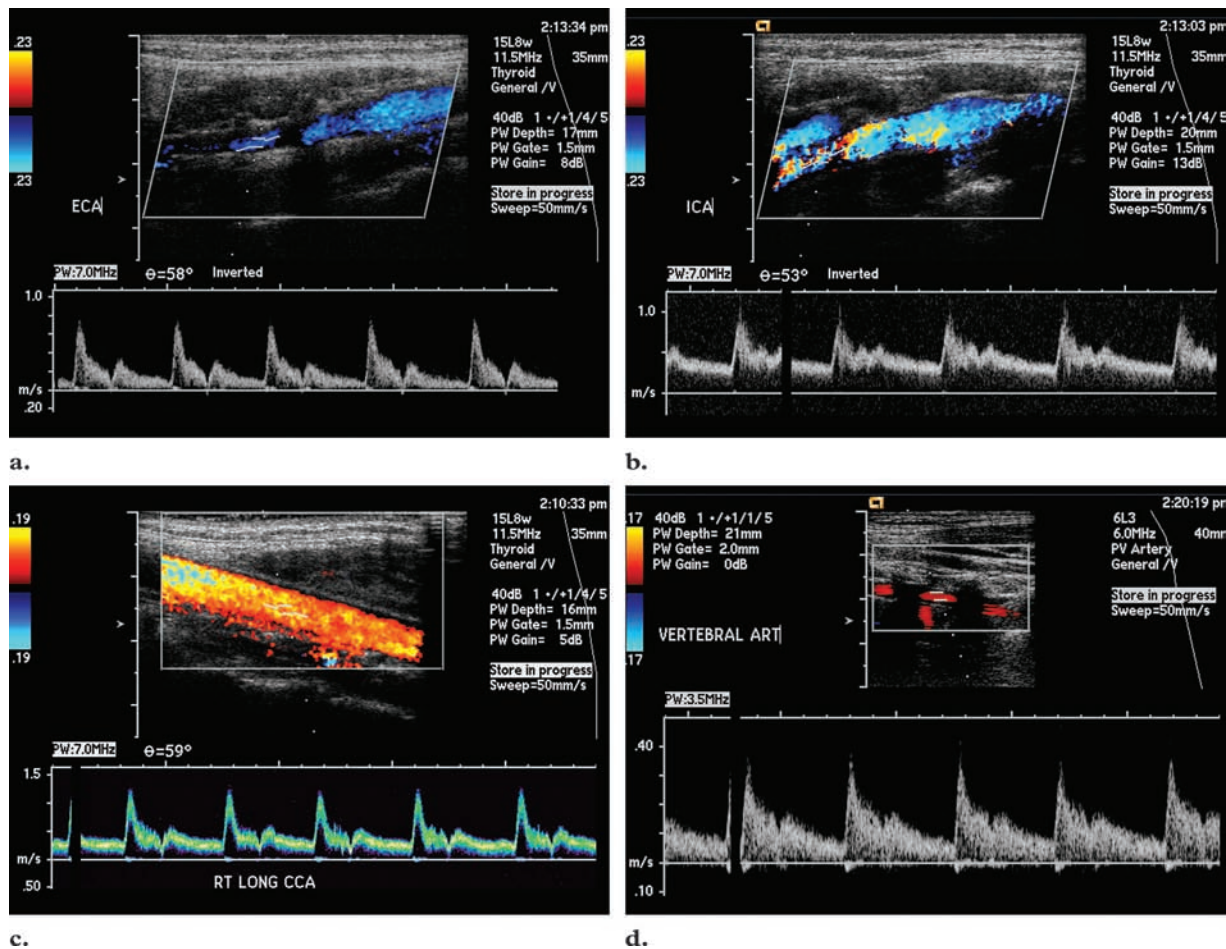
a.

b.

c.

d.

Figure 3. Normal spectral waveforms from major arteries in the neck of a 15-year-old girl. **(a)** Spectrum from the external carotid artery shows a high-resistance waveform with reversal of flow in early diastole. **(b)** Spectrum from the internal carotid artery displays a low-resistance waveform with continuous forward diastolic flow and with a spectral line that ascends farther above the baseline than that from the external carotid artery. **(c)** Spectrum from the common carotid artery represents a composite of waveforms from the external carotid artery and internal carotid artery but more closely resembles the waveform from the internal carotid artery, because 80% of the common carotid artery flow goes into the internal carotid artery. **(d)** Spectrum from the vertebral artery shows low-resistance forward flow above the baseline throughout diastole. Spectral broadening is due to the small diameter of this vessel.

Figure 4. Spectrum from a normal internal jugular vein in a 15-year-old girl shows *a*, S, *v*, and D waves that result from pressure changes in the right atrium.

Internal Carotid Artery

The internal carotid artery supplies low-resistance cerebral circulation. The systolic peak in the waveform from this vessel is not as sharp as that in the waveform from the external carotid artery, and a large quantity of forward flow continues throughout diastole (Fig 3b). In neonates, PSV of 47–73 cm/sec, EDV of 13–21 cm/sec, and RI of 0.64–0.80 have been reported (5). These value ranges differ from those measured in adults (PSV of 62–90 cm/sec, EDV of 23–37 cm/sec, and RI of 0.54–0.66) (4).
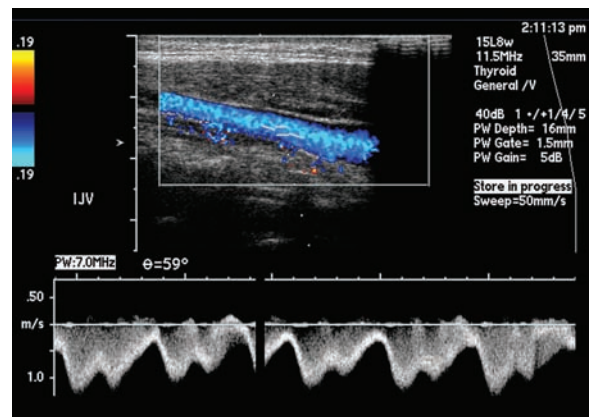
Common Carotid Artery

Spectra obtained in the common carotid artery display components of both internal carotid artery and external carotid artery waveforms but most closely resemble that of the internal
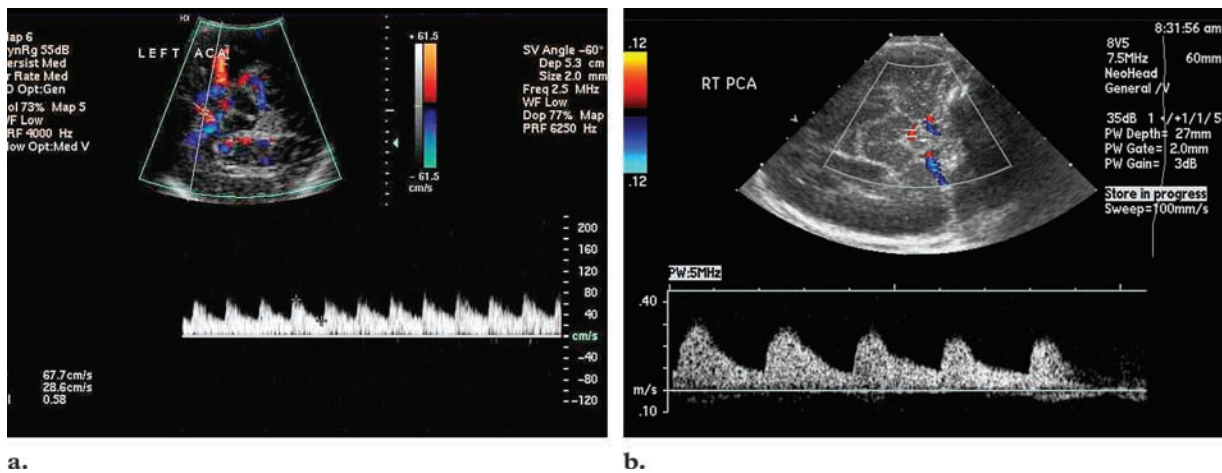
Figure 5.   Normal spectral waveforms from intracranial arteries. **(a)** Spectrum from the anterior cerebral artery in an 8-month-old girl shows a low-resistance waveform with continuous forward diastolic flow. **(b)** Spectrum from the posterior cerebral artery in a 6-day-old girl shows similar low resistance but less diastolic flow than in **a**. Note the complete filling of the spectral window because of the small diameters of these vessels.

carotid artery: Approximately 80% of the flow of the common carotid artery goes to the internal carotid artery, and the diastolic flow is generally above the baseline (6) (Fig 3c). In adults, PSV of 78–118 cm/sec, EDV of 20–32 cm/sec, and RI of 0.72–0.84 have been reported (4).

Vertebral Artery
Spectra obtained in the vertebral artery show a low-resistance flow pattern with continuous flow in systole and diastole (Fig 3d). Since the vessel diameter is small, the spectral line tends to be broader and fill the spectral window. In neonates, the usual values are PSV of 27–57 cm/sec, EDV of 5–11 cm/sec, and RI of 0.73–0.89 (5). In adults, the usual value ranges are PSV of 40–60 cm/sec, EDV of 14–22 cm/sec, and RI of 0.58–0.73 (4,7).

Internal Jugular Vein
Cardiac contractions and intrathoracic pressure changes are reflected in Doppler spectra obtained in the internal jugular vein (Fig 4). During expiration or the Valsalva maneuver, intrathoracic pressure increases, leading to reduced venous return and an increased diameter of the internal jugular vein. Little or no flow is seen at such times. During inspiration, the venous flow is increased as a result of negative intrathoracic pressure and produces a higher-amplitude spectrum (6). S, *v*, D, and *a* waves are normally discernable.

Intracranial Arteries
Cerebral blood flow accounts for 22%–25% of the cardiac output in neonates and 15% of that in adults. In the first 2 or 3 months after birth, complex variations in cerebral hemodynamics

occur in association with changes in pO_2, pCO_2, and ductus arteriosus closure. Both pO_2 and pCO_2 are strong regulators of cerebral blood flow. Vasodilatation is seen with hypoxemia and hypercapnea (8). After the 3rd day of life, there is a gradual increase in PSV and EDV (8).

All intracranial arteries display a low-resistance flow pattern with continuous forward flow during systole and diastole. Because these arteries usually have a diameter of less than 5 mm, the spectral lines are broad and the spectral window is filled. In premature babies, the intracerebral RI is high; an RI of up to 1 may be normal (6). Variations in cerebral blood flow that occur as adaptations to postnatal life are poorly reflected in the RI and PI; hence, they are less informative in the first few months of life (8).

In full-term neonates, the usual value ranges are as follows: in the anterior cerebral artery (Fig 5a), PSV of 12–35 cm/sec, EDV of 6–20 cm/sec, and RI of 0.60–0.80; in the middle cerebral artery, PSV of 20–70 cm/sec, EDV of 8–20 cm/sec, and RI of 0.60–0.80; in the posterior cerebral artery (Fig 5b), PSV of 20–60 cm/sec, EDV of 8–25 cm/sec, and RI of 0.60–0.80; and in the basilar artery, PSV of 30–80 cm/sec, EDV of 5–20 cm/sec, and RI of 0.60–0.80 (6).

Intracranial Veins
Referred cardiac pulsations normally can be seen in the intracranial veins. Venous waveforms in the superior sagittal sinus may be continuous and monophasic or may fluctuate in synchronicity with arterial pulsations (Fig 6) (8). Intracranial venous flow velocities gradually increase after

Teaching Point

Figure 6. Normal spectrum from the superior sagittal sinus in a 10-week-old-boy shows a phasic waveform caused by pulsation from a nearby artery.

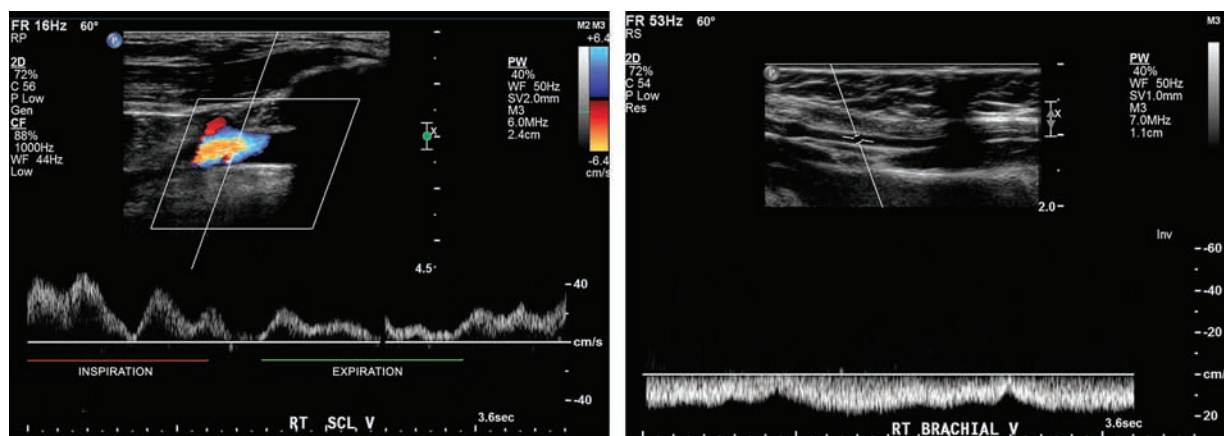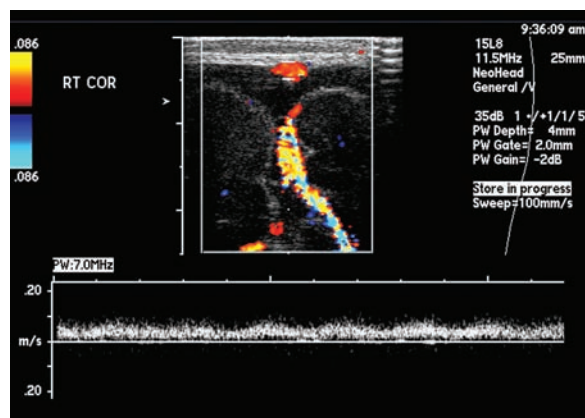a.   b.

Figure 8. Normal spectral waveforms from upper limb veins. **(a)** Subclavian vein waveform in a 5-year-old boy shows the waves produced by right atrial pressure changes. Decreased wave amplitude during expiration and increased amplitude during inspiration also are visible. **(b)** Brachial vein waveform from a 1½-year-old girl shows phasic variation due to respiration and mild undulation due to the back reflection of cardiac pulsations.

birth. The mean velocity in the superior sagittal sinus usually ranges between 8 and 12 cm/sec in neonates (6). However, great variations can be seen in flow velocity with factors such as head rotation, crying, and other activities (9). The transverse sinus usually can be assessed in neonates and shows an intracranial venous flow velocity of 2.7–3.3 cm/sec (6).

Upper Limb Vessels

Upper Limb Arteries
Peripheral vessels such as upper limb arteries show a triphasic flow pattern with strong forward systolic flow followed by a short reversal of flow in early diastole and continuation of the forward flow for a variable length of diastole (Fig 7). Peripheral arteries supply the high-resistance vascular bed of muscles. This high resistance results in early diastolic reversal (second phase) and reduced forward flow in diastole (third phase).

Flow velocities decrease as vessels become smaller. The usual average PSV values in the adult subclavian artery, axillary artery, and brachial artery are 105 cm/sec, 80 cm/sec, and 60 cm/sec, respectively (10). In our experience, lower velocities are seen in children.

Upper Limb Veins
Like the Doppler spectra obtained in neck veins, those obtained in arm veins comprise waves that reflect back-pressure from the right atrium. These a, S, v, and D waves all can be seen in normal Doppler spectra (Fig 8). These waves vary in amplitude during the different phases of respiration: During inspiration, the venous return and spectral amplitude increase because of negative intrathoracic pressure. During expiration, the venous flow velocity decreases. This respiration-related phasic flow pattern is the exact opposite of that in lower limb veins. An absence of right atrial waves from spectra obtained in upper limb veins is indicative of a central venous obstruction (11).
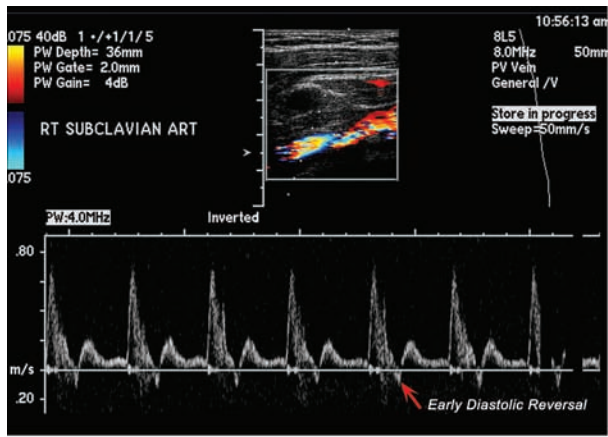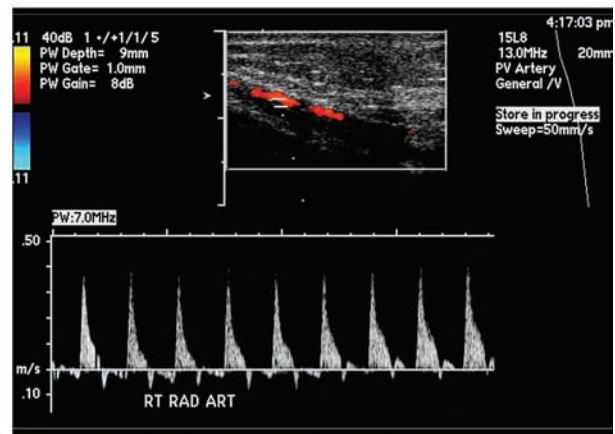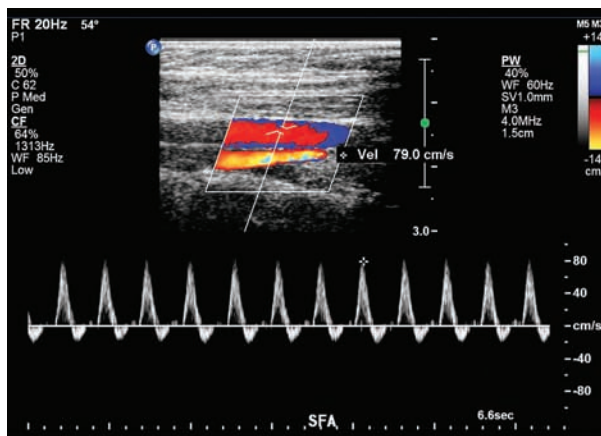
Figure 7. Normal spectral waveforms from upper limb arteries. **(a)** Spectrum from the subclavian artery in a 16-year-old girl shows a triphasic waveform with reversal of flow in early diastole (arrow). **(b, c)** Spectra from subclavian **(b)** and radial **(c)** arteries in an 11-week-old boy show triphasic waveforms similar to that in **a** but with less diastolic flow, a finding indicative of higher resistance.
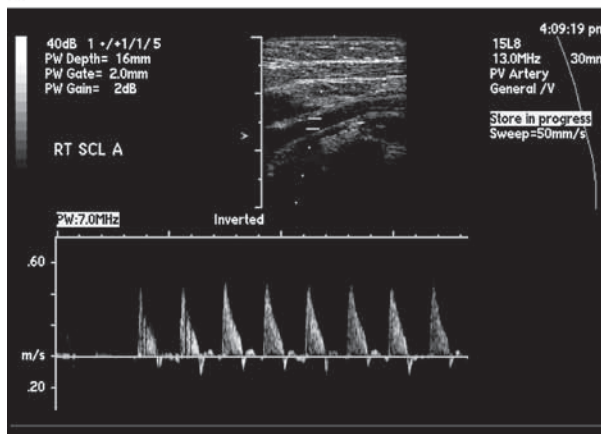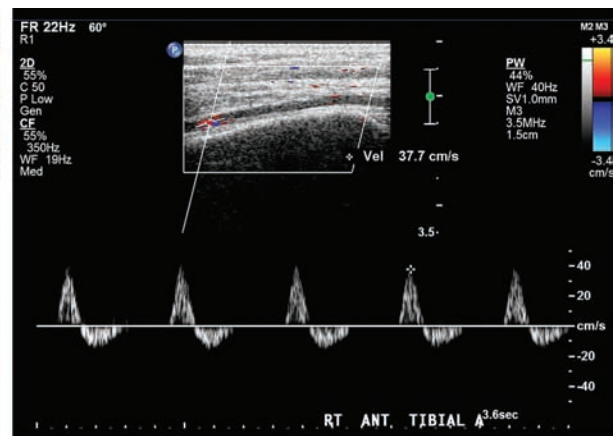

Figure 9. Normal spectral waveforms from lower limb arteries. **(a)** Spectrum from the superficial femoral artery in a 5-year-old boy shows a triphasic waveform with diastolic reversal and little forward diastolic flow. **(b)** Spectrum from the anterior tibial artery in a 14-year-old girl shows high resistance with almost no forward flow in diastole.

Lower Limb Vessels

Lower Limb Arteries

Triphasic high-resistance waveforms are seen in lower limb arteries as in other peripheral arteries (Fig 9). Normal flow velocities for adult common femoral, superficial femoral, popliteal, and tibioperoneal arteries are in the range of 100 cm/sec, 80–90 cm/sec, 70 cm/sec, and 40–50 cm/sec, respectively (6).

Figure 10. Normal spectral waveforms from lower limb veins. **(a)** Common femoral vein waveform obtained during breath holding in an 11-year-old boy shows *a*, S, *v*, and D waves. **(b)** Waveform from the popliteal vein in an 11-year-old boy shows a reduced flow velocity during inspiration and an increased velocity during expiration. **(c)** Posterior tibial vein waveform from an 11-year-old boy shows phasic variations from respiration with mild superimposed undulation from right atrial pressure changes.
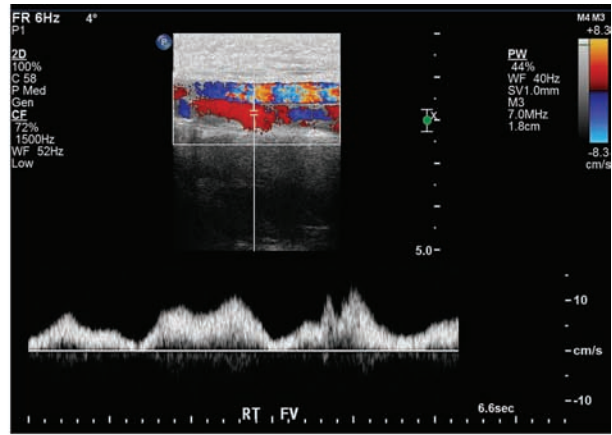
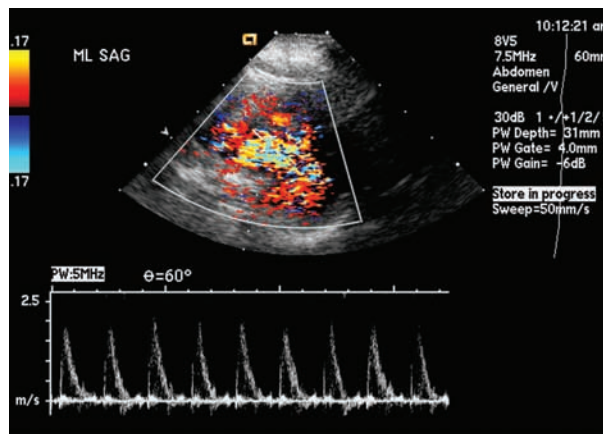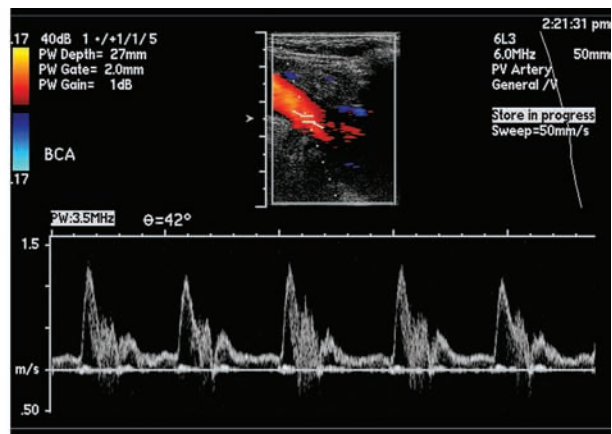**Figure 11.** Normal Doppler spectra from the major thoracic arteries. **(a)** Spectrum from the ascending aorta in an 8-year-old boy shows a triphasic waveform with a sharp systolic peak and narrow spectral line. **(b)** Spectrum from the brachiocephalic artery in a 15-year-old girl shows a triphasic waveform with early diastolic reversal and a good amount of forward flow in late diastole.
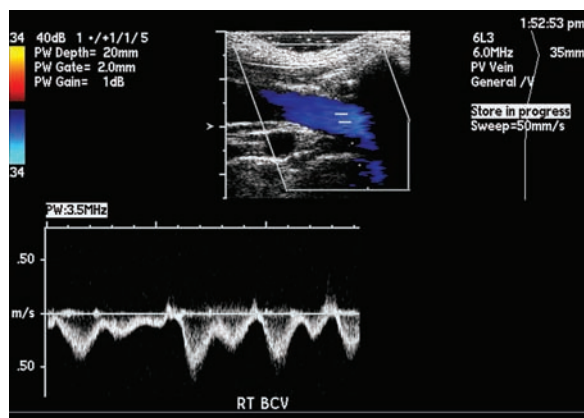
Figure 12.   Normal Doppler spectrum from the brachiocephalic vein in a 4-year-old girl shows *a*, S, *v*, and D waves from pressure changes in the right atrium, as well as reduced flow velocity during expiration.
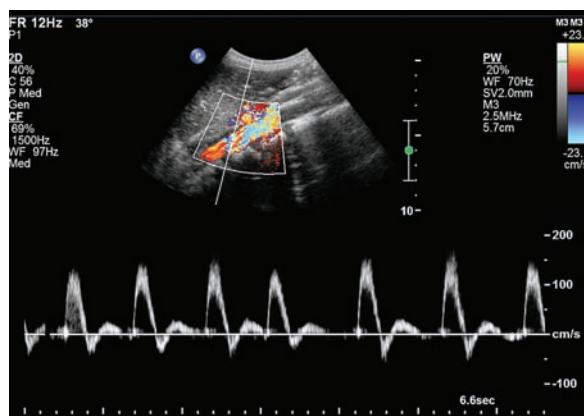

Figure 13.   Normal Doppler spectrum from the upper abdominal aorta in a 10-year-old boy shows a typical waveform characterized by a sharp increase in antegrade flow velocity during systole, followed by a reversal of flow in early diastole and then low-velocity antegrade flow in the remainder of diastole.

Lower Limb Veins

The phasic pattern of flow in lower limb veins reflects a combination of both cardiac and respiratory movements (3). Normally, all four waves that represent right atrial changes can be seen in the spectral line (Fig 10). If the S, *v*, and D waves are completely above the baseline and the *a* wave is either completely above the baseline or descends less than 5 cm/sec below it, normal antegrade flow is considered to be present. A deeper descent of the *a* wave below the baseline is indicative of retrograde or pulsatile flow, a pattern suggestive of increased right atrial pressure (12).

During inspiration, increased intraabdominal pressure results in a reduction of venous return from the lower limbs, which in turn leads to a decrease in the velocity or amplitude of the wave-

form. During expiration, flow velocities in the lower limb veins increase (3). The maximum flow velocity in femoral veins in adults is 12–30 cm/sec (13).

Thoracic Vessels

Ascending Aorta
Flow through the aorta produces a triphasic waveform with early diastolic reversal. The systolic peaks are sharp, with a narrow spectral line (Fig 11a). PSV in the ascending aorta in children is reported to be 98–143 cm/sec (14).

Brachiocephalic Artery
The brachiocephalic artery supplies blood to the low-resistance cerebral vascular bed as well as to the high-resistance vascular bed in muscles of the neck and upper extremities. This function of the artery is reflected in spectral waveforms that are triphasic, with an early diastolic reversal (Fig 11b).

Superior Vena Cava
Spectral waveforms obtained in the superior vena cava show phasic changes due to back-pressure from the right atrium and changes in amplitude with respiration. The *a*, S, *v*, and D waves all are visible. In the superior vena cava, flow velocity increases with inspiration, as negative intrathoracic pressure increases the venous return, and decreases with expiration. Maximum flow velocity in the superior vena cava in children is 60–80 cm/sec (15). In young adults, the reported maximum value is 32–69 cm/sec (16).

Brachiocephalic Vein
Spectra obtained in the brachiocephalic vein are characterized by waveforms and respiration-related changes similar to those seen in spectra from the superior vena cava (Fig 12).

Abdominal and Pelvic Vessels

Abdominal Aorta and Iliac Arteries
The normal Doppler flow pattern in the aorta is that of plug flow. In the aorta and iliac arteries, the flow is typically high resistance, with a sharp increase in antegrade flow velocity during systole followed by a rapid decrease that bottoms out in early diastole with a brief period of reversed flow (Fig 13). Low-velocity antegrade flow then
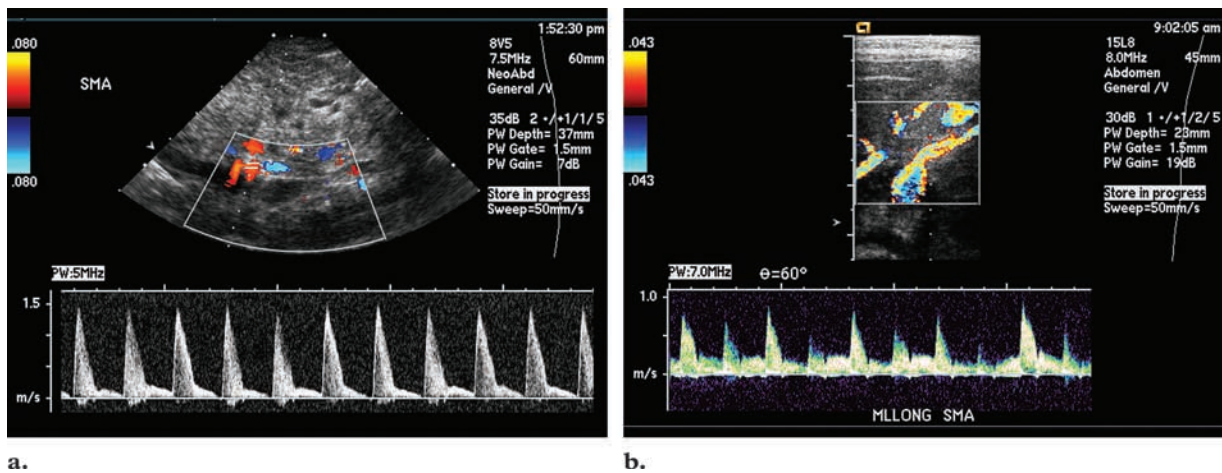
a.   b.

Figure 14.   Normal spectral waveforms in the superior mesenteric artery. **(a)** Fasting waveform from a 26-day-old neonate shows a high-resistance flow pattern. **(b)** Postprandial waveform from a 6-day-old neonate shows a low-resistance pattern with an increase in diastolic flow velocity.

resumes and continues for the remainder of diastole. Spectral Doppler analysis shows that the peak antegrade velocity decreases and the amount of retrograde flow increases as the flow progresses from the proximal aorta to the iliac vessels (17).

Celiac Trunk and Superior Mesenteric Artery

The celiac artery has a high-resistance pattern at its origin, with a small amount of reversed flow in early diastole. Its distal portion and branches lose the reversed early-diastolic flow component, showing continuous low-resistance forward flow throughout the cardiac cycle (17).

With the body in a fasting state, flow through the superior mesenteric artery has a high-resistance pattern, with a small amount of reversed flow in early diastole (Fig 14a). After a meal, the PSV and diastolic velocities increase. The reversed diastolic flow disappears, a low-resistance pattern develops, and the systolic spectral peak broadens (17) (Fig 14b).

Inferior Vena Cava and Iliac Veins

The waveform of the inferior vena cava varies according to the specific segment sampled. The flow in the proximal inferior vena cava is influenced by the activity of the right atrium and shows back-pressure changes identical to those seen in hepatic venous flow (18) (Fig 15). Distally, the cardiac activity has a lesser effect on flow velocities, and variations in thoracic or
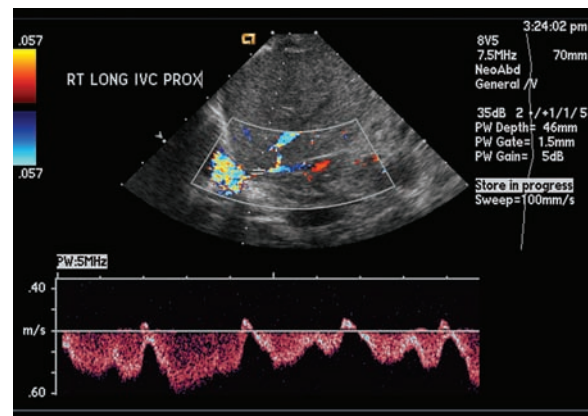

Figure 15.   Normal Doppler spectrum from the intrahepatic portion of the inferior vena cava in a 4-day-old boy shows the waves that result from right atrial back-pressure.

abdominal pressure cause greater variability in forward flow (18). In the common iliac veins, the flow pattern is more phasic, like that seen in the proximal lower limb veins (17).

Hepatic Vessels

Hepatic Veins.—Most people have three hepatic veins: left, middle, and right. However, accessory hepatic veins are commonly observed. The hepatic veins join the inferior vena cava immediately inferior to the diaphragm and are in open communication with the right side of the heart (19). Flow in the hepatic veins is predominantly hepatofugal (away from the liver, toward the inferior vena cava) (20). The Doppler spectral waveforms from normal hepatic veins are multiphasic, similar to those obtained in the inferior vena cava
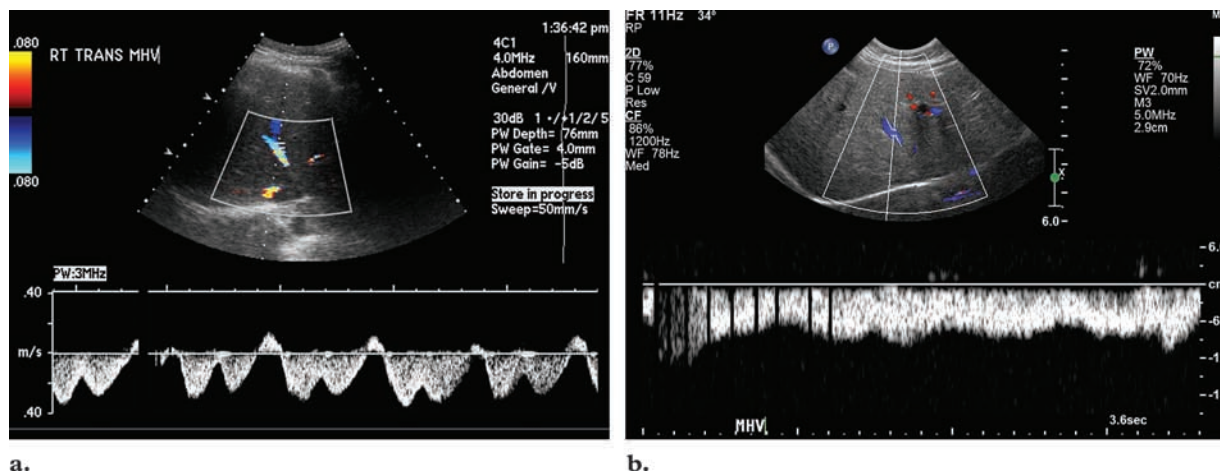
Figure 16.   Normal spectral waveforms obtained in hepatic veins. **(a)** Spectrum from the middle hepatic vein in a 17-year-old girl shows normal *a*, S, *v*, and D waves from right atrial pressure changes. **(b)** Spectrum from the middle hepatic vein in a 1-month-old girl shows a normal monophasic flow pattern.
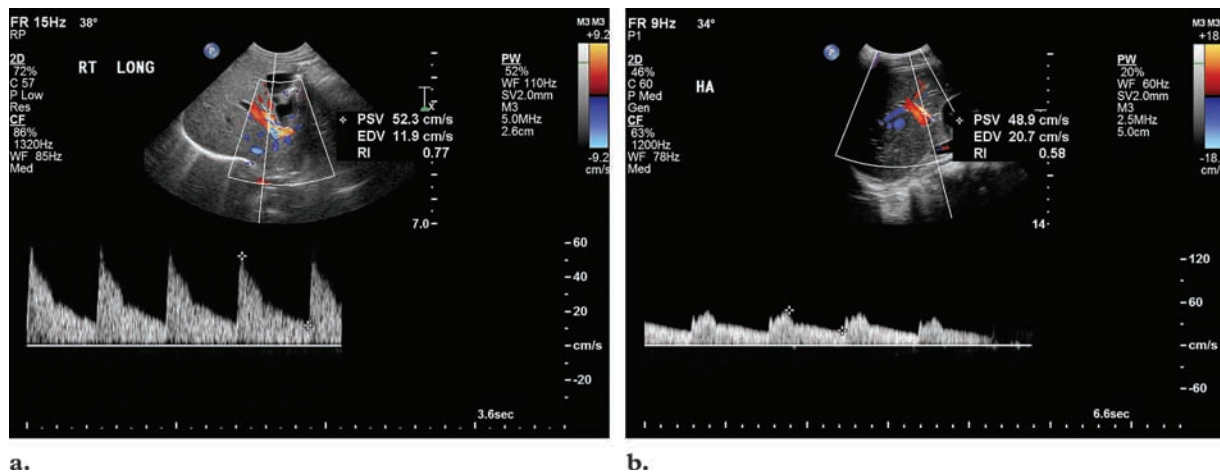

Figure 17.   Normal spectral waveforms from different segments of the hepatic artery. **(a)** Spectrum from the hepatic artery at the porta hepatis in a 4-day-old girl demonstrates low-resistance and high-velocity diastolic flow. **(b)** Spectrum from the left branch of the hepatic artery in a 13-year-old boy shows lower resistance than that in **a**. The calculated RI also was lower.

and other large systemic veins (21). The waveform in the normal hepatic vein consists of two large antegrade waves (toward the heart) that represent atrial diastole and ventricular systole; a small retrograde wave (away from the heart) that represents flow during atrial systole; and a small wave between the two antegrade waves, which is produced by overfilling of the right atrium (19,21) (Fig 16a).

The monophasic flow pattern sometimes seen in neonates (Fig 16b) is normal and may be secondary to atypical hepatic compliance due to a large horizontally positioned liver or to hepatic hematopoietic activity (22). Variations in flow pattern among the veins have been reported. Flow in the middle hepatic vein has the most

consistent triphasic pattern, probably because this vein is positioned at a favorable angle for Doppler US (22). There is no variation in triphasic activity after a meal (22).

Hepatic Artery.—The direction of blood flow in the hepatic artery is hepatopetal (toward the liver). Hepatic artery waveforms demonstrate low resistance and high diastolic flow velocities (20) (Fig 17a). Normal hepatic arterial PSV in a fasting adult patient is approximately 30–40 cm/sec, and EDV is 10–15 cm/sec (19). The normal RI in

a fasting patient varies from 0.55 to 0.81 (mean, 0.62–0.74). There is a consensus that the RI increases after a meal and also with age (19,23). The RI is higher at the porta hepatis (Fig 17a) and lower in vessel branches closer to the periphery of the liver (24) (Fig 17b).

Portal Vein.—The direction of normal portal venous flow is hepatopetal. The flow velocity is fairly uniform, although slight variations may occur in the spectral line because of respiration (Fig 18). Some degree of periodicity or pulsatility resulting from cardiac activity also has been observed in normal portal veins (19). The mean portal venous flow velocity in a fasting adult is approximately 18 cm/sec (range, 13–23 cm/sec) (19). The volume and velocity of portal venous flow normally increase after meals (25,26), reflecting the increased flow in the superior mesenteric artery (25). The splenic vein and the superior mesenteric vein show Doppler flow patterns similar to that of the portal vein (27).

Renal Vessels

Renal Arteries.—Arterial flow in the main renal vessels and within the renal parenchyma demonstrates a prominent systolic peak, with antegrade diastolic flow present throughout the cardiac cycle (28) (Fig 19). The normal PSV in adults is 100–180 cm/sec, and the normal EDV is 25–50 cm/sec (29). The normal ratio of renal artery PSV to aortic PSV is less than 3.5 (18,30).

   The intraparenchymal RI may be useful in the evaluation of renal disease. Doppler waveforms should be obtained from the arcuate arteries (at the corticomedullary junction) or interlobar arteries (adjacent to the medullary pyramids) (31). The renal arterial RI varies markedly over the 1st year of life. Preterm infants normally may have a renal arterial RI value as high as 0.9, although neonates and infants less than 1 year old generally have an RI of 0.6–0.8 and older children (ages ≥1 year) have an RI of 0.5–0.7 (18,32) (Fig 19b). The physiologic and anatomic immaturity of the neonatal kidney accounts for these differences. At birth, the active plasma renin gradually increases, while the renal blood flow rate, glomerular filtration rate, and tubular excretory capacity of sodium all decrease. Adult levels are reached after the first 6 months to 1 year of life (32).

Figure 18. Spectral waveform from the portal vein in a 10-year-old boy shows a typical flow pattern, with fairly uniform velocity and slight phasic variations due to respiration and cardiac motion.

Renal Veins.—The flow in the renal veins is generally continuous, but mild fluctuations may be seen as a reflection of respiration and right atrial contraction (18,28) (Fig 20).

Ovarian Vessels

The ovary receives blood from the aorta via the main ovarian artery and adnexal branches of the uterine artery. The intraovarian arteries are coiled and change in diameter according to the level of follicular activity. The venous system roughly parallels the arterial system, a pampinifom plexus that directly connects to the gonadal veins. The right ovarian vein drains directly into the inferior vena cava, and the left ovarian vein drains into the left renal vein (33). It may be difficult to detect flow at Doppler US even in normal ovaries (34). The waveforms of normal intraovarian arteries typically show low flow velocities (Fig 21). In arteries in the ovary without the dominant follicle, there is a pattern of relatively high resistance, whereas in the active ovary, both during ovulation and during the formation of the corpus luteum, there is a pattern of low resistance with a continuous antegrade arterial flow throughout diastole (35–37). Decreased resistance in arteries in the active ovary is thought to be secondary to hormone-mediated changes in vascular compli-
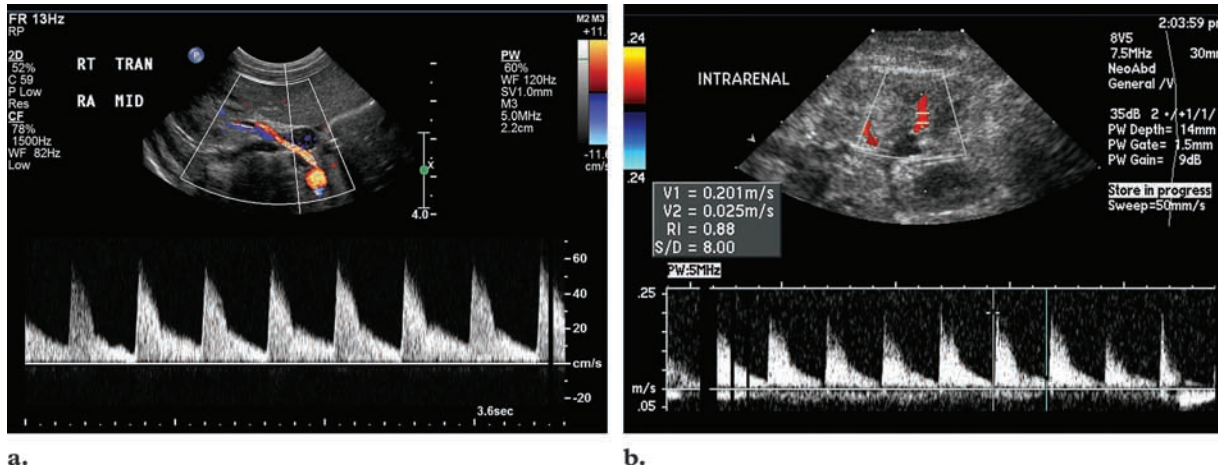
Teaching Point

Teaching Point

a.   b.

Figure 19.   Normal spectral waveforms from renal arteries. **(a)** Spectrum from the midportion of the right renal artery in a 2-day-old girl demonstrates a prominent systolic peak, with antegrade flow throughout diastole. **(b)** Spectrum from an intraparenchymal renal artery in a preterm 26-day-old girl shows relatively high resistance (RI of 0.88), which is considered normal for preterm neonates.
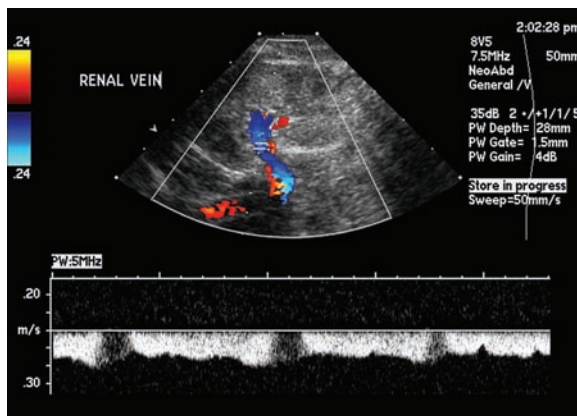

Figure 20.   Spectrum from a normal renal vein in a 26-day-old girl shows continuous flow with minimal variations secondary to respiration and right atrial pressure changes.
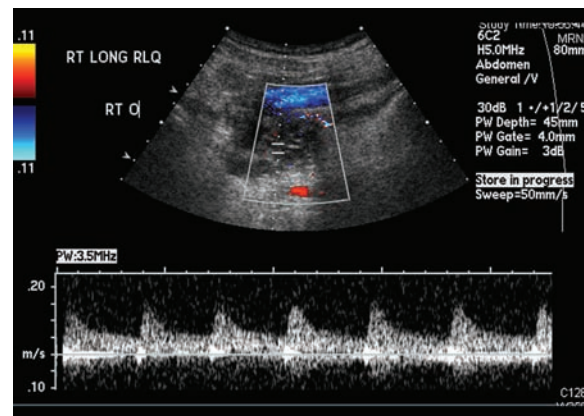

Figure 21.   Spectrum from a normal intraovarian artery in an 11-year-old girl shows low-resistance flow and a low PSV.

ance. The result is an increase in blood flow to the ovary between the late follicular phase and the early luteal phase (38).

Testicular Vessels

The testicular arteries arise from the anterior aspect of the aorta, just distal to the renal arteries, and provide the primary vascular supply to the testes (39). The testicular arteries divide into branches that pierce the tunica albuginea and course along the periphery of the testis in a layer

known as the tunica vasculosa. These capsular arteries supply centripetal branches that enter the testicular parenchyma and course toward the mediastinum (40). The blood supply to the testicular parenchyma is supplemented via transmediastinal arteries that course from the mediastinum to the testicular parenchyma (41).

The spectral waveform produced by flow through the intratesticular arteries characteristically has a low-resistance pattern (40). The reported
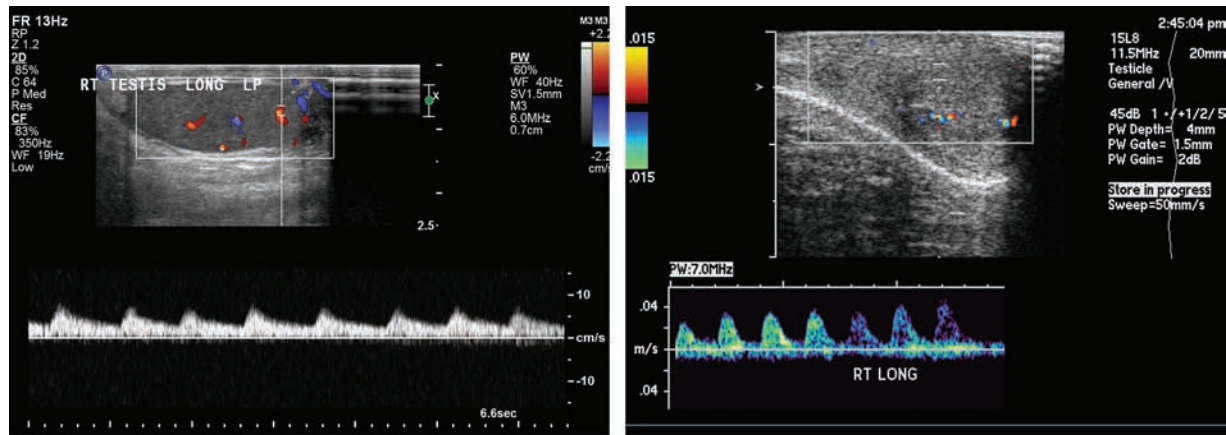
a.   b.
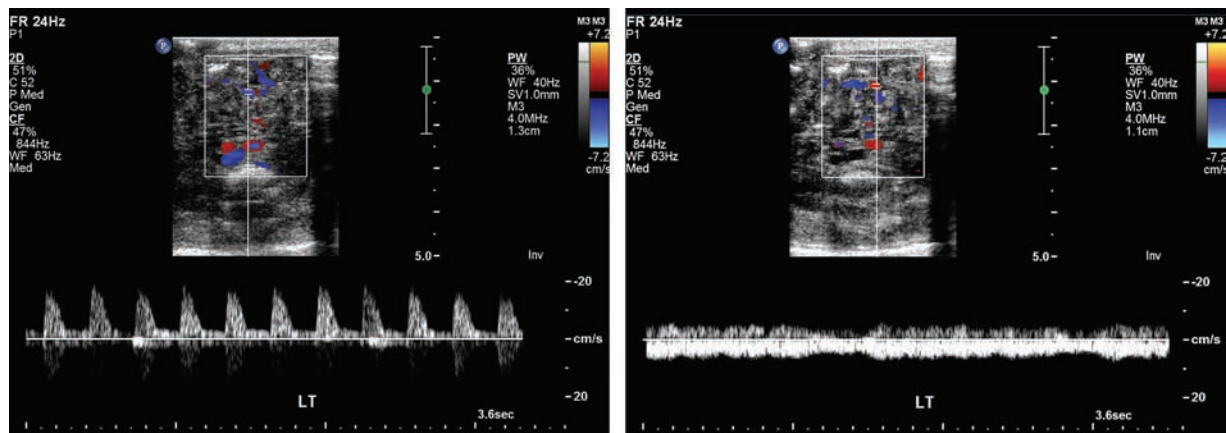
Figure 22.   Spectra from intratesticular arteries in children. **(a)** Waveform obtained in a 12-year-old boy shows a normal low-resistance flow pattern. **(b)** Waveform obtained in a 2-month-old boy with a testicular volume of 0.7 cm^3 shows higher resistance than in **a**, a finding considered normal in a child of this age. The calculated RI also was higher than that in **a**.

a.   b.

Figure 23.   Arterial **(a)** and venous **(b)** spectral waveforms obtained in the bowel wall of an 18-day-old girl show normal perfusion.

normal testicular values in healthy young adults are as follows: RI of 0.48–0.75 (mean, 0.62), PI of 0.7–2.3 (mean, 1.3), PSV of 4.0–19.5 cm/sec (mean, 9.7 cm/sec), and EDV of 1.6–6.9 cm/sec (40) (Fig 22a). In prepubertal testicles (with a volume of less than 4 cm^3), the diastolic arterial flow may not be detectable (42,43), and the RI tends to be higher than in pubertal and postpubertal testes (44) (Fig 22b). These differences may be explained by vasodilatation and increased blood flow in mature testes (44).

Bowel Vessels

Color Doppler US is useful for assessing bowel viability in patients with suspected or proved necrotizing enterocolitis (45). Bowel perfusion in normal neonates, as demonstrated at color Doppler US by using a velocity setting of 8.6 cm/sec, ranged from one to nine color dots per square centimeter (45). To our knowledge, no studies have been published about Doppler spectra in the setting of normal bowel vascularity. However, in our experience, both arterial (Fig 23a) and venous (Fig 23b) spectra may be obtained in the bowel wall.

Summary

Each major vessel in the human body has a characteristic Doppler spectral waveform that reflects the physiologic need of the organ it supplies and the position of the vessel relative to the heart. Arterial flow may be characterized either as monophasic, with forward (antegrade) diastolic flow supplying the low-resistance vascular beds of solid organs such as the brain, kidney, and liver, or triphasic, with reversed diastolic flow supplying high-resistance vascular beds such as those of the skeletal muscles. The Doppler spectra of all major veins show back-pulsations from right atrial pressure changes during the cardiac cycle, as well as variations in amplitude (velocity) caused by the alternation of respiratory phases. The most significant difference between Doppler spectra obtained in children and those obtained in adults is the high RI seen in neonates, especially premature babies, not only in vessels supplying solid organs such as the brain and kidneys but also in peripheral arteries.

References

1. Nelson TR, Pretorius DH. The Doppler signal: where does it come from and what does it mean? AJR Am J Roentgenol 1988;151:439–447.
2. Taylor KJ, Holland S. Doppler US. I. Basic principles, instrumentation, and pitfalls. Radiology 1990;174:297–307.
3. Abu-Yousef MM, Mufid M, Woods KT, Brown BP, Barloon TJ. Normal lower limb venous Doppler flow phasicity: is it cardiac or respiratory? AJR Am J Roentgenol 1997;169:1721–1725.
4. Yazici B, Erdogmus B, Tugay A. Cerebral blood flow measurements of the extracranial carotid and vertebral arteries with Doppler ultrasound in healthy adults. Diagn Interv Radiol 2005;11:195–198.
5. Kehrer M, Golez R, Schoning M. The development of hemodynamics in the extracranial carotid arteries of healthy preterm and term neonates. Ultrasound Med Biol 2004;30:283–287.
6. Carroll BA. The extracranial cerebral vessels. In: Rumack CM, Wilson SR, Charboneau JW, Johnson J, eds. Diagnostic ultrasound. 3rd ed. St. Louis, Mo: Elsevier Mosby, 2005; 943–992.
7. Scheel P, Ruge C, Schoning M. Flow velocity and flow volume measurements in the extracranial carotid and vertebral arteries in healthy adults: reference data and the effect of age. Ultrasound Med Biol 2000;26:1261–1266.
8. Couture AP. Normal neonatal brain: colour Doppler and pulsed Doppler. In: Couture A, Veyrac C, eds. Transfontanellar Doppler imaging in neonates. Heidelberg, Germany: Springer, 2001; 9–90.
9. Dean LM, Taylor GA. The intracranial venous system in infants: normal and abnormal findings on duplex and color Doppler sonography. AJR Am J Roentgenol 1995;164:151–156.
10. Taneja K, Jain R, Sawhney S, Rajani M. Occlusive arterial disease of the upper extremity: colour Doppler as a screening technique and for assessment of distal circulation. Australas Radiol 1996;40: 226–229.
11. Patel MC, Berman LH, Moss HA, McPherson S. Subclavian and internal jugular veins at Doppler US: abnormal cardiac pulsatility and respiratory phasicity as a predictor of complete central occlusion. Radiology 1999;211:579–583.
12. Abu-Yousef MM, Kakish ME, Mufid M. Pulsatile venous Doppler flow in lower limbs: highly suggestive of elevated right atrium pressure. AJR Am J Roentgenol 1996;167:977–980.
13. Alimoglu E, Erden A, Gursel K, Olcer T. Correlation of right atrium pressure and blood flow velocities in common femoral vein obtained by duplex Doppler sonography. J Clin Ultrasound 2001;29: 87–91.
14. Poutanen T, Tikanoja T, Sairanen H, Jokinen E. Normal aortic dimensions and flow in 168 children and young adults. Clin Physiol Funct Imaging 2003;23:224–229.
15. Ayabakan C, Ozkutlu S. Normal patterns of flow in the superior caval, hepatic and pulmonary veins as measured using Doppler echocardiography during childhood. Cardiol Young 2003;13:143–151.
16. Appleton CP, Hatle LK, Popp RL. Superior vena cava and hepatic vein Doppler echocardiography in healthy adults. J Am Coll Cardiol 1987;10: 1032–1039.
17. Downey D. The retroperitoneum and great vessels. In: Rumack CM, Wilson SR, Charboneau JW, Johnson J, eds. Diagnostic ultrasound. 3rd ed. St. Louis, Mo: Elsevier Mosby, 2005; 443–487.
18. Coley BD. Pediatric applications of abdominal vascular Doppler. Part II. Pediatr Radiol 2004;34: 772–786.
19. Martinez-Noguera A, Montserrat E, Torrubia S, Villalba J. Doppler in hepatic cirrhosis and chronic hepatitis. Semin Ultrasound CT MR 2002;23: 19–36.
20. Paltiel HJ. Pediatric abdominal applications of color Doppler ultrasonography. Ultrasound Q 2002;18: 161–185.
21. Abu-Yousef MM. Duplex Doppler sonography of the hepatic vein in tricuspid regurgitation. AJR Am J Roentgenol 1991;156:79–83.
22. Jequier S, Jequier JC, Hanquinet S, Gong J, Le Coultre C, Belli DC. Doppler waveform of hepatic veins in healthy children. AJR Am J Roentgenol 2000;175:85–90.
23. Joynt LK, Platt JF, Rubin JM, Ellis JH, Bude RO. Hepatic artery resistance before and after standard meal in subjects with diseased and healthy livers. Radiology 1995;196:489–492.
24. Lafortune M, Patriquin H. The hepatic artery studies using Doppler sonography. Ultrasound Q 1999;15:9–26.

25. Coley BD. Pediatric applications of abdominal vascular Doppler imaging. Part I. Pediatr Radiol 2004; 34:757–771.
26. Kao SC, Bell EF, Brown BP, Smith WL. Duplex Doppler sonography of changes in portal vein flow in healthy term newborn infants after feeding. J Ultrasound Med 1996;15:121–125.
27. Gallix BP, Taourel P, Dauzat M, Bruel JM, Lafortune M. Flow pulsatility in the portal venous system: a study of Doppler sonography in healthy adults. AJR Am J Roentgenol 1997;169:141–144.
28. Thurston W, Wilson S. The urinary tract. In: Rumack CM, Wilson SR, Charboneau JW, Johnson J, eds. Diagnostic ultrasound. 3rd ed. St Louis, Mo: Elsevier Mosby, 2005; 321–393.
29. Radermacher J. Ultrasonography in the diagnosis of renovascular disease. Imaging Decis MRI 2002; 6:15–22.
30. Lee HY, Grant EG. Sonography in renovascular hypertension. J Ultrasound Med 2002;21:431–441.
31. Tublin ME, Bude RO, Platt JF. Review. The resistive index in renal Doppler sonography: where do we stand? AJR Am J Roentgenol 2003;180:885–892.
32. Bude RO, DiPietro MA, Platt JF, Rubin JM, Miesowicz S, Lundquist C. Age dependency of the renal resistive index in healthy children. Radiology 1992; 184:469–473.
33. Fleischer AC, Brader KR. Sonographic depiction of ovarian vascularity and flow: current improvements and future applications. J Ultrasound Med 2001;20:241–250.
34. Surratt J, Siegel M. Imaging of pediatric ovarian masses. RadioGraphics 1991;11:533–548.
35. Fleischer AC, Rodgers WH, Kepple DM, Williams LL, Jones HW 3rd, Gross PR. Color Doppler sonography of benign and malignant ovarian masses. RadioGraphics 1992;12:879–885.
36. Taylor KJ, Burns PN, Woodcock JP, Wells PN. Blood flow in deep abdominal and pelvic vessels: ultrasonic pulsed-Doppler analysis. Radiology 1985;154:487–493.
37. Pellizzari P, Esposito C, Siliotti F, Marchiori S, Gangemi M. Colour Doppler analysis of ovarian and uterine arteries in women with hypoestrogenic amenorrhoea. Hum Reprod 2002;17:3208–3212.
38. Schiller VL, Grant EG. Doppler ultrasonography of the pelvis. Radiol Clin North Am 1992;30: 735–742.
39. Dogra VS, Gottlieb RH, Oka M, Rubens DJ. Sonography of the scrotum. Radiology 2003;227: 18–36.
40. Middleton WD, Thorne DA, Melson GL. Color Doppler ultrasound of the normal testis. AJR Am J Roentgenol 1989;152:293–297.
41. Middleton WD, Bell MW. Analysis of intratesticular arterial anatomy with emphasis on transmediastinal arteries. Radiology 1993;189:157–160.
42. Atkinson GO Jr, Patrick LE, Ball TI Jr, Stephenson CA, Broecker BH, Woodard JR. The normal and abnormal scrotum in children: evaluation with color Doppler sonography. AJR Am J Roentgenol 1992;158:613–617.
43. Bader TR, Kammerhuber F, Herneth AM. Testicular blood flow in boys as assessed at color Doppler and power Doppler sonography. Radiology 1997;202:559–564. [Published correction appears in Radiology 1997;203:580.]
44. Paltiel HJ, Rupich RC, Babcock DS. Maturational changes in arterial impedance of the normal testis in boys: Doppler sonographic study. AJR Am J Roentgenol 1994;163:1189–1193.
45. Faingold R, Daneman A, Tomlinson G, et al. Necrotizing enterocolitis: assessment of bowel viability with color Doppler US. Radiology 2005;235: 587–594.

Normal Doppler Spectral Waveforms of Major Pediatric Vessels: Specific Patterns

Govind B. Chavhan, MD, DNB, et al

Page 692

Each normal major vessel in the human body has a characteristic flow pattern that is representable in spectral waveforms obtained with Doppler ultrasonography (US) and that reflects both the anatomic position of the vessel and the physiologic need of the organ it supplies.

Page 692

The RI and the PI provide information about blood flow and resistance that cannot be obtained from measurements of absolute velocity alone. The effects of variation in vessel angulation and size are nullified in the calculation of these indexes.

Page 695

In premature babies, the intracerebral RI is high; an RI of up to 1 may be normal. Variations in cerebral blood flow that occur as adaptations to postnatal life are poorly reflected in the RI and PI; hence, they are less informative in the first few months of life.

Page 702

The renal arterial RI varies markedly over the 1st year of life. Preterm infants normally may have a renal arterial RI value as high as 0.9, although neonates and infants less than 1 year old generally have an RI of 0.6–0.8 and older children (ages 1 year) have an RI of 0.5–0.7. The physiologic and anatomic immaturity of the neonatal kidney accounts for these differences. At birth, the active plasma renin gradually increases, while the renal blood flow rate, glomerular filtration rate, and tubular excretory capacity of sodium all decrease. Adult levels are reached after the first 6 months to 1 year of life.

Page 702

In arteries in the ovary without the dominant follicle, there is a pattern of relatively high resistance, whereas in the active ovary, both during ovulation and during the formation of the corpus luteum, there is a pattern of low resistance with a continuous antegrade arterial flow throughout diastole.